

# Crack propagation in and fractography of epoxy resins

SALIM YAMINI, ROBERT J. YOUNG

*Department of Materials, Queen Mary College, Mile End Road, London, UK*

The relationship between the stability of crack propagation in, and the fracture surface appearance of, DGEBA epoxy resins cured with TETA has been investigated using a linear elastic fracture mechanics approach. In particular, the effect of varying the amount of curing agent and curing conditions and altering external variables such as testing rate, temperature and environment have been studied. Under certain conditions, propagation is found to be stable and fracture surfaces have a smooth appearance. Under other conditions the cracks propagate in an unstable "stick-slip" manner. In this case, arrest lines can be seen on the fracture surfaces and their intensity and roughness increases with the magnitude of the crack jumps. The roughness of the fracture surfaces has been measured using a Talysurf and this has been shown to be due principally to deviation of the cracks from the original fracture plane rather than any gross plastic deformation.

## 1. Introduction

Epoxy resins are being used increasingly in structural applications such as matrix materials in high-performance composites and adhesives in the aerospace industry. Because of this, the prediction of the strength of such components is of vital importance. Such predictions are normally made for brittle materials using linear elastic fracture mechanics [1] and this approach has been widely used for brittle polymers such as polymethylmethacrylate [2–4]. However, with epoxy resins, much of the effort has been concerned with crack propagation in adhesive test pieces [5–10] and, until recently, propagation in the resin alone had not received so much attention [11–16]. It is now apparent that before crack propagation in the adhesive case can be understood, crack propagation in the resin alone must be fully characterized.

Reports of the crack propagation behaviour of epoxy resins have sometimes appeared to be inconsistent in themselves [14] and to contradict the work of others [15, 17, 18]. Many of these problems have stemmed from the widely reported observation that epoxy resins are prone to crack propagation on some occasions by means of a continuous (stable) mode and at other times by a crack jumping (unstable or "stick-slip") mode

[11–15]. Continuous crack propagation gives rise to a smooth load-displacement curve during propagation whereas "stick-slip" propagation leads to the characteristic "saw-tooth" curve illustrated schematically in our recent publications [19, 20].

The stability of crack propagation is known to vary with the type and amount of curing agent, environment and testing rate [11, 19, 20]. It has also recently become clear that specimen geometry can exert an influence upon crack propagation in materials that are prone to unstable propagation [9, 17]. The fracture surface morphologies of epoxy resins have also received relatively little attention and there have been few attempts to correlate them with the crack propagation behaviour. Phillips *et al.* [16] have recently examined the effect of temperature and testing rate upon the fracture surface morphologies of an epoxy resin cured with two different series of amine hardeners. They found a considerable difference in morphology between fracture surfaces of resins cured with primary amines and those cured with mixed amines. They also found that for one particular system, the fracture surface changes in appearance when the testing rate or testing temperature are changed.

Although the phenomenon of crack propagation in epoxy resins is now at least partially understood, there have been no successful attempts to explain the reasons for the wide variations in crack propagation behaviour and fracture surface appearance and no successful explanations of the underlying failure mechanisms. The reason for this is probably that the conditions under which each type of crack propagation behaviour and surface morphology are found have not been properly identified and this makes any formulation of a theoretical explanation rather difficult. It is the purpose of this present investigation, by concentrating upon one particular resin and hardener system, to identify at least some of the variables which control the crack propagation behaviour and the formation of different surface features. Of the particular variables, we have chosen to vary hardener content, post-curing temperature and period, testing temperature and environment, in conjunction with a systematic variation of the testing rate. The effects of different curing agents and specimen thickness and the relationship between crack propagation and yield behaviour have also been studied and the results published previously [19, 20].

## 2. Experimental details

### 2.1. Specimen preparation

The resin used for the crack propagation specimens was a commercial diglycidyl ether of bisphenol A (DGEBA), Epikote 828 (Shell) cured with triethylene tetramine (TETA), a mixed primary and secondary amine. The details of the preparation of the sheets have been given in a recent publication [20]. Different quantities of the hardener were used: 7.4, 9.8, 12.3, 14.7 and 17.3 phr\*. In all cases, the initial hardening reaction was allowed to proceed for 24 h at room temperature followed by post-curing at elevated temperatures and subsequent slow-cooling to room temperature.

The specimens for crack propagation experiments were cut in the form of rectangular plates, approximately 3.7 mm × 30 mm × 60 mm, from the cast sheets. They were notched at one end and a V-shaped groove, about 0.5 mm deep, was made along the centre of one face. To ensure that the cracks would propagate centrally along the specimens, a sharp blade was pressed into and run along the groove.

### 2.2. Double torsion testing

Crack propagation was studied using the double torsion (DT) testing geometry which has been described in detail elsewhere [3]. The DT test is particularly useful for crack propagation studies since it uses a "linear compliance" specimen and the stress intensity factor,  $K_{IC}$ , is independent of crack length,  $c$ , and for an elastic material, is given by [21]

$$K_{IC} = P_c W_m \left[ \frac{(1 + \nu)}{W t^3 t_n k_1} \right]^{1/2} \quad (1)$$

where  $P_c$  is the applied load,  $W_m$  is the moment arm (10.4 mm),  $\nu$  is Poissons ratio (assumed to be constant for an epoxy resin at 0.35 [20]),  $W$  is the specimen width (30 mm),  $t$  is the specimen thickness (3.7 mm) and  $t_n$  is the thickness of the plate in the plane of the crack.  $k_1$  is a constant which depends on the ratio  $(W/2)/t$  and is  $\frac{1}{3}$  when this ratio is infinity [21]. In our case  $(W/2)/t$  is about 4 and  $k_1$  has been taken as 0.282.

The DT specimens were tested in an Instron mechanical testing machine under compressive loading using a constant cross-head speed ( $\dot{y}$ ) for each specimen. Under these conditions it can be shown that when propagation is stable

$$\dot{y} = B P_c \dot{c} = \text{constant}, \quad (2)$$

where  $B$  is the slope of the compliance calibration curve for the specimen and  $\dot{c}$  is the crack velocity. In epoxy resins, crack propagation is mainly unstable and generally occurs in a "stick-slip" manner. In this case, the crack is stationary during loading and at some critical load jumps, first accelerating to a high velocity and then slowing down to become stationary again. Consequently, there is a simple relationship between crack velocity and cross-head displacement rate in this case.

### 2.3. Examination of fracture surfaces

The two broken halves of the DT specimens used for crack propagation studies were taken for examination of their fracture surfaces. Micrographs of the fracture surfaces were taken at various magnifications using reflected light optical microscopy. In the specimens which showed the "stick-slip" behaviour, each crack jump and arrest event manifested itself as a crack arrest line on both fracture surfaces. Each arrest line could be correlated with a peak on the load-displacement

\* phr – parts by weight of hardener per 100 parts by weight of resin.

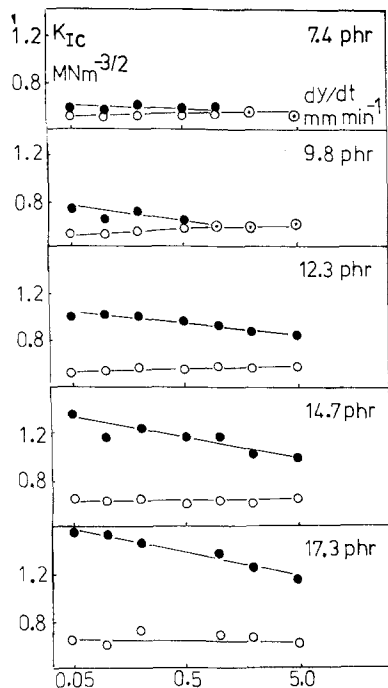


Figure 1 Variation of  $K_{ICi}$  and  $K_{ICa}$  with cross-head speed in Epikote 828 specimens with different stated amounts of TETA hardener, post-cured for 3 h at  $100^\circ\text{C}$  and tested at room temperature.  $\bullet$   $K_{ICi}$ ,  $\circ$   $K_{ICa}$ ,  $\odot$   $K_{IC}$  continuous. (These symbols for  $K_{IC}$  are used in all the figures).

curve. The arrest lines seemed to have a ridged appearance but due to perceptual difficulties it was impossible to tell whether these ridges were above or below the fracture plane in either half of the specimen and knowledge of this is crucial to the understanding of the “stick–slip” process. Because of the problems with perception Talysurf\* traces of both fracture surfaces of each sample were obtained. A Talysurf is a device which detects the roughness of a surface by means of a stylus which runs along the surface. In this present work, the stylus was always run along the length of the fracture surfaces, half way between the top and bottom surfaces of the specimens. In order to minimize any mismatch in the traces of the two surfaces of a sample as far as possible, the stylus was run along identical paths on each half of the same sample.

### 3. Results

#### 3.1. Curing agent content

Crack propagation in the epoxy resin cured with different amounts of TETA curing agent and post-

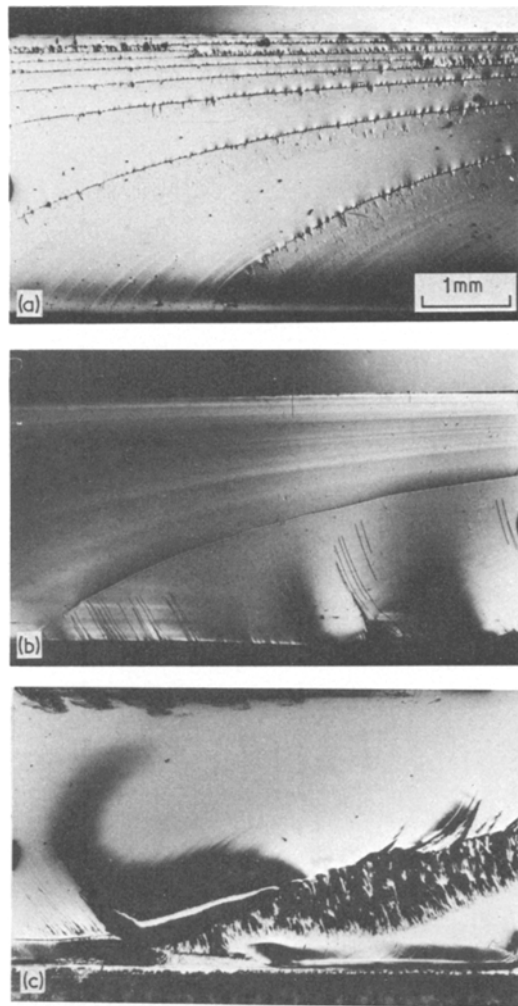


Figure 2 Fracture surfaces of Epikote 828 specimens differing in amount of TETA hardener, post-cured for 3 h at  $100^\circ\text{C}$  tested at room temperature at cross-head speed of  $0.05\text{ mm min}^{-1}$ ; (a) 7.4, (b) 9.8, (c) 17.3 phr.

cured for 3 h at  $100^\circ\text{C}$  was studied at  $22 \pm 2^\circ\text{C}$  using a range of cross-head displacement rates. The effect of changing these variables is illustrated in Fig. 1.  $K_{ICi}$  and  $K_{ICa}$  are the critical stress intensity factors for initiation and arrest, respectively, and the difference between them characterizes the amount of jumping which has taken place. When the difference is large, propagation occurs by means of large jumps, whereas when it is small, the jumps are small, and when  $K_{ICi}$  is equal to  $K_{ICa}$ , propagation is continuous. In all cases it was found that the tendency for cracks to jump increased as the curing agent content was increased and the cross-head speed reduced. However, the value of

\* Talysurf 4 is made by The Rank Organization, Rank, Taylor Hobson Division, Leicester, UK.

$K_{ICa}$  remained roughly constant when either the cross-head speed or curing agent content were varied.

Micrographs of fracture surfaces of samples with 7.4, 9.8 and 17.3 phr curing agent are shown in Fig. 2. They are all of fracture surfaces of samples tested at a cross-head speed of  $0.05 \text{ mm min}^{-1}$ . The well-defined curved lines are crack arrest lines. The direction of crack propagation in the DT specimen is perpendicular to the arrest line and not parallel to the top and bottom specimens surfaces. As the curing agent content is increased the arrest lines appear to become better defined and broader. The arrest lines on the fracture surface of the sample with the lowest curing agent content (Fig. 2a) are very thin and at high magnification can be seen to have triangular features along them. The triangular features are absent in the fracture surfaces of samples with higher amounts of curing agent (Fig. 2b and c). In Fig. 2b, there are some irregularly spaced fine markings which are parallel to the direction of crack propagation. They can also be seen in Fig. 2c immediately ahead of the broad crack arrest region. The fracture surfaces of samples which failed by continuous crack propagation are relatively smooth, but they did sometimes show the irregularly spaced fine markings (micrographs not shown). Another feature which can be noticed on some surfaces is the occurrence of secondary arrest lines. These lines are rather poorly defined and their density appears to decrease as the amount of curing agent is increased. As with the main arrest lines, they also have a similar curved profile but are featureless and are difficult to resolve in the optical microscope. A schematic diagram of the fracture surface in Fig. 2b is given in Fig. 3 so that the different features on the micrographs can be clearly distinguished from one another.

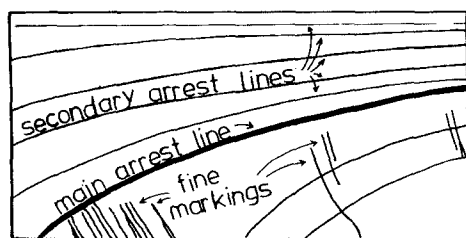


Figure 3 Schematic diagram of the fracture surface Fig. 2b showing various features.

### 3.2. Post-cure temperature

The effect of different post-curing temperatures upon the stability of crack propagation over a range of cross-head speeds at  $22 \pm 2^\circ \text{C}$  is shown in Fig. 4. All the specimens contained 9.8 phr curing agent and had been post-cured for 3 h. Samples which had been post-cured at  $50^\circ \text{C}$  (Fig. 4a) failed in a similar manner irrespective of cross-head speed. However, crack propagation in samples which had been post-cured at 100 and  $150^\circ \text{C}$  (Fig. 4b and c) showed an increasing tendency to undergo large jumps. The jumps were the largest in the specimens cured at  $150^\circ \text{C}$  and tested at the lowest cross-head speeds. Again  $K_{ICa}$  did not appear to change and was virtually constant for all cross-head speeds and post-curing temperatures.

Fig. 5 shows optical micrographs of the fracture surfaces of samples post-cured at  $50^\circ \text{C}$  (Fig. 5a) and  $150^\circ \text{C}$  (Fig. 5b). Both of these samples were tested at  $5 \text{ mm min}^{-1}$ . More magnified micrographs of these two surfaces are shown in Fig. 5c and d. The micrograph of the sample post-cured at the lowest temperature (Fig. 5a) resembles that of the sample with the lowest amount of curing agent and cured at  $100^\circ \text{C}$  (Fig. 2a). The arrest lines in both cases are poorly defined and have triangular

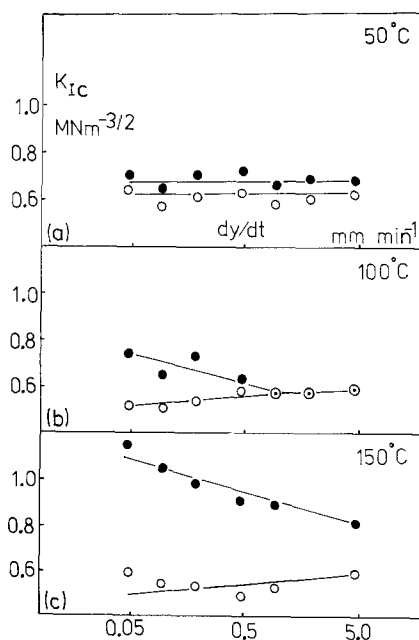


Figure 4 Variation of  $K_{ICi}$  and  $K_{ICa}$  with cross-head speed in Epikote 828 specimens with 9.8 phr TETA hardener post-cured for 3 h at different stated temperatures, all tested at room temperature: (a)  $50^\circ \text{C}$ , (b)  $100^\circ \text{C}$ , (c)  $150^\circ \text{C}$ .

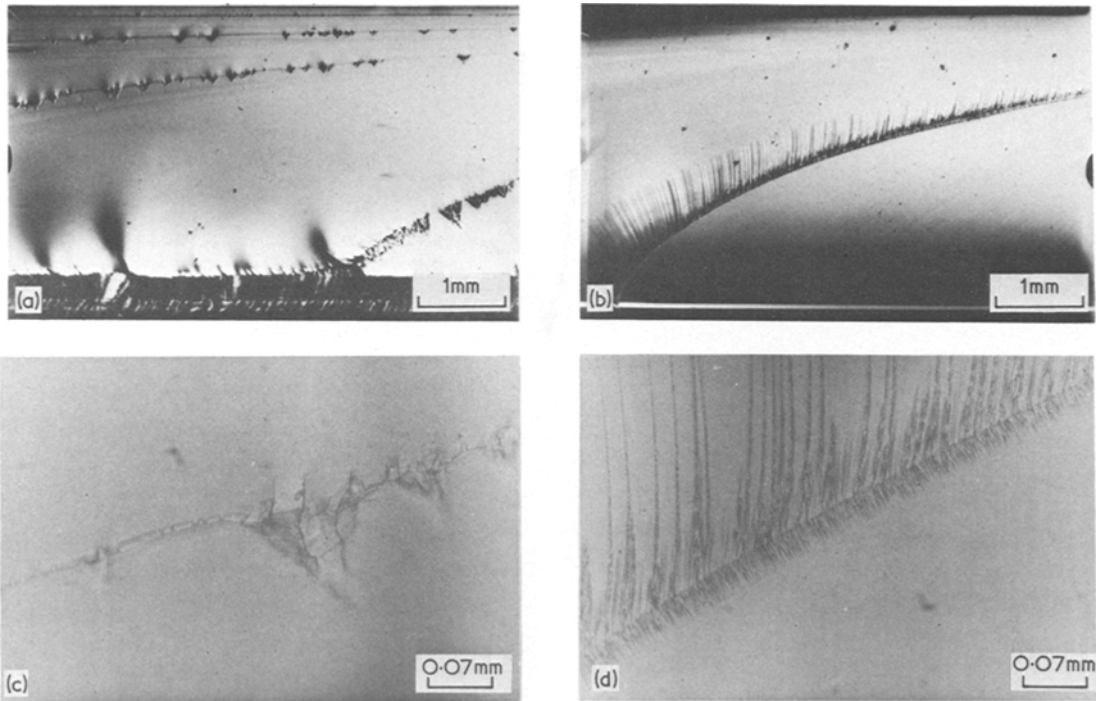


Figure 5 Fracture surfaces of Epikote 828 specimens with 9.8 phr TETA hardener, cured for 3 h, tested at room temperature at cross-head speed of  $5 \text{ mm min}^{-1}$ , differing in post-cured temperature: (a) 50, (b) 150° C, (c) more magnified micrograph of (a), (d) more magnified micrograph of (b).

features along them. A magnified view of the triangular features is shown in Fig. 5c. As the post-cure temperature is increased, the line becomes more defined and hackled (Fig. 5b and d). There is some evidence for secondary arrest lines in the micrographs in Fig. 5, but they appear to be rather faint and poorly defined.

### 3.3. Post-cure period

The effect of post-curing period upon crack propagation at different cross-head speeds at  $22 \pm 2^\circ \text{ C}$  is shown in Fig. 6. In this case, all the specimens contained 9.8 phr curing agent and had been post-cured at  $100^\circ \text{ C}$ . From Fig. 6 it can be seen that increasing the post-curing period beyond about 3 h does not significantly alter the crack propagation behaviour, at least when a post-cure temperature of  $100^\circ \text{ C}$  is employed. However, it can be seen that increasing the post-cure period up to 3 h tends to cause larger crack jumps. For all post-cure times used there was a transition at about  $0.5 \text{ mm min}^{-1}$  from unstable to stable propagation on increasing the cross-head displacement rate.

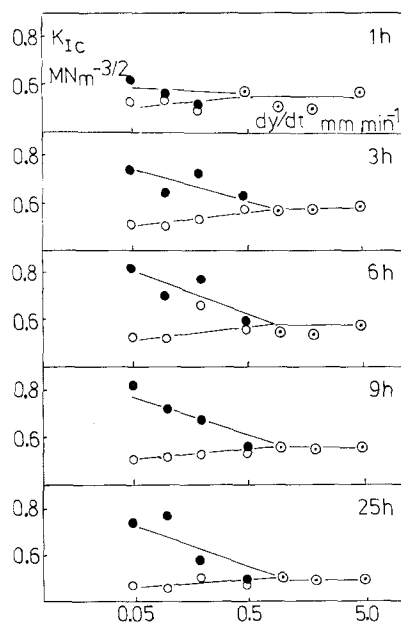


Figure 6 Variation of  $K_{ICi}$  and  $K_{ICa}$  with cross-head speed in Epikote 828 specimens with 9.8 phr TETA post-cured at  $100^\circ \text{ C}$  for different stated curing periods, all tested at room temperature.

Micrographs of fracture surfaces of the samples post-cured for various periods at 100° C and tested at the same cross-head speed were very similar to that in Fig. 2b.

### 3.4. Testing temperature

The effect of testing temperature upon crack propagation in the resin cured with 9.8 phr TETA and post-cured for 3 h at 100° C was also studied. The variation of  $K_{ICi}$  and  $K_{ICa}$  with testing temperature at a cross-head speed of 0.5 mm min<sup>-1</sup> has been shown elsewhere [20]. At this particular cross-head speed, crack propagation is continuous below about 10° C (283 K) whereas above this temperature, crack jumping occurs and the jumps become larger as the test temperature is increased. All the specimens were precracked at room temperature, so that they contained sharp cracks, before they were tested at the various temperatures. At high temperatures, the jumps were so large that  $K_{ICa}$  could not be measured because cracks did not arrest within the specimens.

The effect of cross-head speeds upon the stability of crack propagation was also studied at three different temperatures, i.e. -43, +22 67° C (Fig. 7). At -43° C crack propagation was found to be entirely continuous over the entire range of cross-head speeds used. However, at the

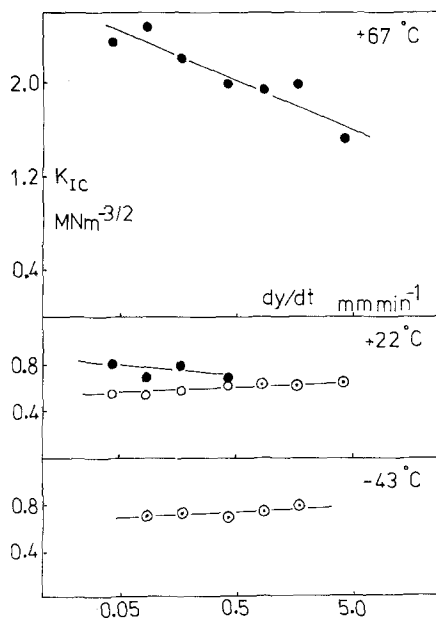


Figure 7 Variation of  $K_{ICi}$  and  $K_{ICa}$  with cross-head speed in Epikote 828 specimens with 9.8 phr TETA, post-cured at 100° C for 3 h, tested at different stated temperatures.

other two temperatures, jumping occurred and, as before, the value of  $K_{ICi}$  increased with decreasing cross-head speed.

Micrographs of the fracture surfaces of samples tested at -50, 22 and 60° C are shown in Fig. 8. At -50° C, where propagation was entirely by a continuous mode, the fracture surface is smooth and featureless (Fig. 8a). The fracture surface of the specimen tested at 22° C (Fig. 8b and also shown in Fig. 2b) has a well-defined arrest line, secondary arrest lines and irregularly spaced fine markings. At 60° C a sharp arrest line is observed on the fracture surface, followed by a broad rough hackled region (Fig. 8c).

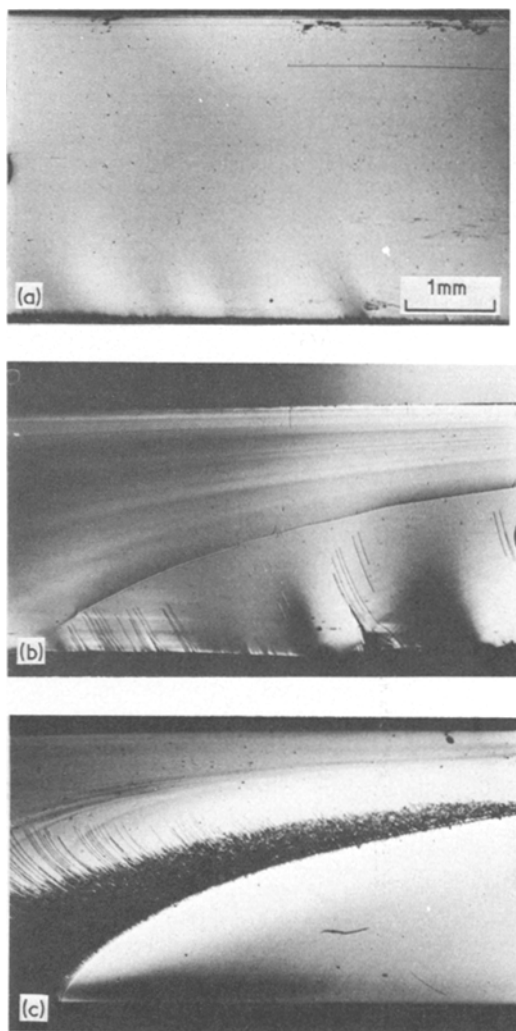


Figure 8 Fracture surfaces of Epikote 828 specimens with 9.8 phr TETA post-cured at 100° C for 3 h using different testing temperatures. (a) -50, (b) +22, (c) +60° C. (a) and (c) are tested at cross-head speed of 0.5 mm min<sup>-1</sup> and (b) at 0.05 mm min<sup>-1</sup>.

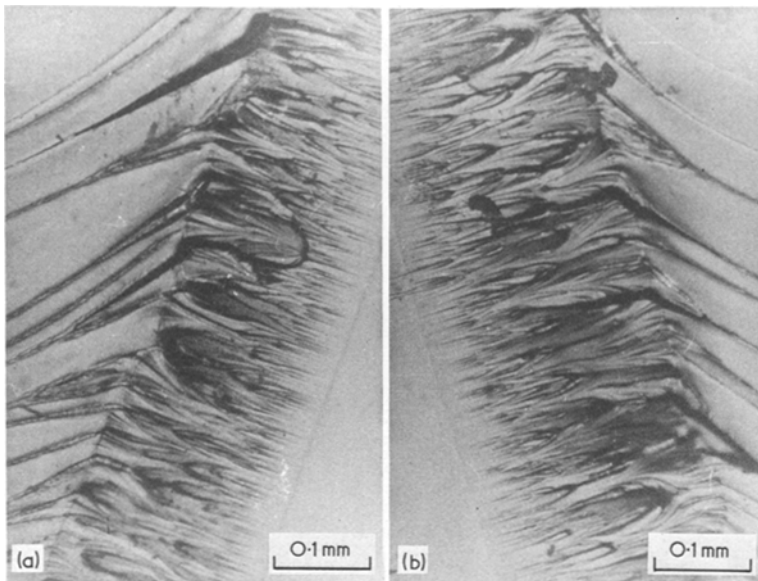


Figure 9 Micrographs of the fracture surfaces of the two halves of a sample (Epikote 828 + 14.7 phr TETA post-cured at 100° C for 3 h, tested at room temperature at cross-head speed of 0.5 mm min<sup>-1</sup>) showing features along a main crack arrest line.

### 3.5. Effect of water

The effect of testing the specimens in water upon the stability of crack propagation in the resin cured with 9.8 phr TETA was also investigated. The variation of  $K_{ICi}$  and  $K_{ICa}$  for this system tested in distilled water, with cross-head speed, is given in [20]. The effect of water is to suppress continuous propagation and cause jumping to occur over the entire range of cross-head speeds used. Because of the tendency of water to cause crack jumping, an attempt was made to see if the absence of water would promote stable crack propagation. This was done by propagating cracks under vacuum and it was found that jumping was not suppressed. The details of this experiment have been given in a recent publication [20].

The fracture surfaces of samples tested in either air or water appeared to be very similar when

propagation occurred by the same mode. When propagation took place by means of jumping, well-defined arrest lines could be seen on the surfaces, whereas after continuous propagation, the surfaces were smooth and virtually featureless.

### 3.6. Talysurf measurements

Crack arrest lines on the two different halves of the same sample always look identical when examined under the optical microscope as is shown, for example, in Fig. 9. Both halves seem to have ridged arrest lines but it is difficult to say from visual examination whether the ridges are above or below the fracture plane on either half. A less magnified micrograph of the surface of one half of a specimen and Talysurf traces of both surfaces are shown in Fig. 10. The magnification of the micrograph and the horizontal magnification

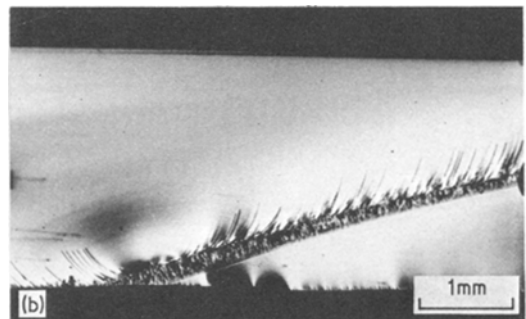
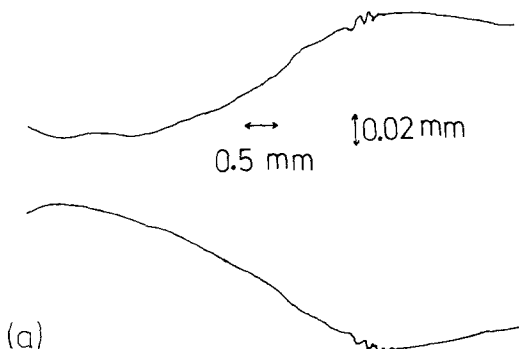


Figure 10 (a) Talysurf traces of the fracture surfaces of two halves of a sample (Epikote 828 + 14.7 phr TETA, post-cured at 100° C for 3 h, tested at room temperature at cross-head speed of 0.5 mm min<sup>-1</sup>). (b) Optical micrograph of one of the fracture surfaces used for traces in (a). The other fracture surface appears identical.

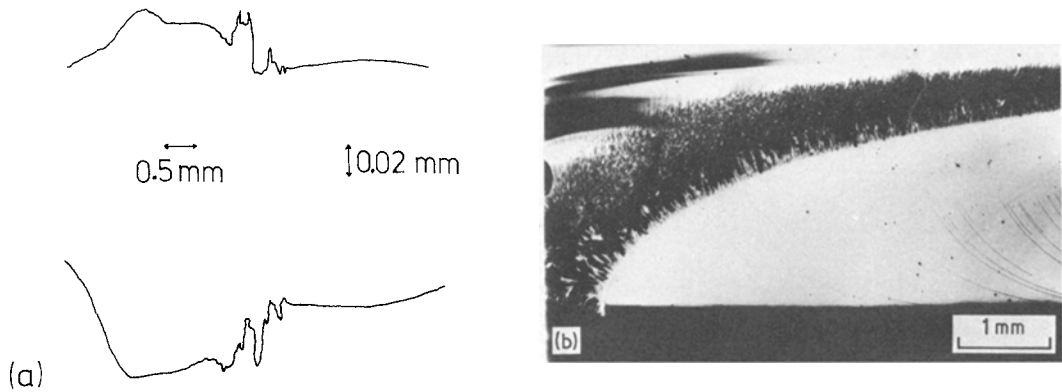


Figure 11 (a) Talysurf traces of the fracture surfaces of two halves of a sample (Epikote 828 + 9.8 phr, post-cured at 100° C for 3 h, tested at cross-head speed of 0.5 mm min<sup>-1</sup> at testing temperature of + 60e C). (b) Optical micrograph of one of the fracture surfaces used for traces in (a). The other fracture surface appears identical.

of the Talysurf traces are approximately the same. It can be seen that the profile of one trace appears to be the mirror image of the other. The small zig-zag parts of the traces correspond to the stylus traversing the crack arrest line.

Another optical micrograph and pair of Talysurf traces is given in Fig. 11. Again the traces were taken from the fracture surfaces of two halves of the same sample and they appear to be mirror images of each other. The traces clearly indicate that the fracture surface up to the arrest line is relatively smooth and then there is a sharp transition to a rough region which can also be seen on the micrograph. When the crack reaches the arrest line it also changes to a different plane which is above the main fracture plane on one half of the specimen and below it on the other half. This means that if the two fracture surfaces were put back together they would interlock. After the rough region, the crack starts to turn back to the original fracture plane. Examination of Talysurf traces of many different fracture surfaces has shown that this type of behaviour is typical of cracks propagating in epoxy resins. The tendency for cracks to deviate from the main fracture plane is illustrated schematically in Fig. 12. A similar type of behaviour was suggested by Phillips *et al.* [16] from the observation of fracture surfaces,



Figure 12 Schematic drawing of profile of crack arrest line in epoxy specimens showing deviation of crack line from main fracture plane (after Phillips *et al.* [16]).

but we felt that since the surfaces of two halves of a specimen appeared identical additional information, such as that which can be provided by the Talysurf, was needed before the model could be substantiated. It is felt that the results of this present work give strong support to the model.

#### 4. Discussion

It has been shown that many factors control the stability of crack propagation in epoxy resins and, subsequently, affect the appearance of the fracture surfaces of specimens. Previous work has shown that the propagation behaviour will be different with different types of curing agent [16, 20]. Using DGEBA cured with TETA it has been found that stable continuous crack propagation is promoted by increasing the rate of testing and decreasing the testing temperature and the absence of liquid water. In addition to testing conditions affecting crack propagation, it has been shown that the amount and type of curing agent and state of cure can also affect propagation. Stable crack growth is found using low amounts of curing agent, low post-curing temperatures and short post-curing periods. Under all other circumstances cracks propagate in an unstable “stick-slip” manner.

It is possible to make some general observations concerning the relationship between fracture surface morphologies and the type of crack propagation that is found. The appearance of fracture surfaces of specimens which have undergone stable continuous crack growth is typified by Fig. 8a. The surface is smooth and relatively featureless. It is rather similar to fracture surfaces of polymethylmethacrylate after crack propagation has taken



place by slow stable crack growth [22]. In a recent publication, it was shown by the authors and co-workers [19] that continuous crack propagation in epoxy resins could be explained in terms of a constant crack opening displacement ( $\delta$ ) criterion as was found previously for polymethylmethacrylate [2, 4]. The similarity between the fracture surfaces in the two cases would seem to strengthen this suggestion. A constant  $\delta$  criterion was found to be inapplicable to epoxy resins during “stick–slip” propagation [19], and again the appearance of the fracture surfaces in this case would appear to be consistent with the earlier investigations. For example, it was found that at low temperatures ( $<10^\circ\text{C}$ ) propagation tended to be continuous with  $\delta$  constant with temperature, but above about  $10^\circ\text{C}$ ,  $\delta$  increased rapidly as the testing temperature was increased [19]. In the present work, it has been shown that the size and roughness of the crack arrest lines increases as the test temperature is increased (Fig. 8). This would be consistent with an increasing crack opening displacement,  $\delta$ .

There also appears to be a general correlation between the size and intensity of the crack arrest lines and the magnitude of the crack jumps (typified by the difference between  $K_{\text{ICi}}$  and  $K_{\text{ICa}}$ ). For example, the roughest and most pronounced crack arrest lines which are shown in Fig. 2c correspond to high values of  $K_{\text{ICi}}$  in Fig. 1. It is assumed that these high values of  $K_{\text{IC}}$  will correspond to high values of  $G_{\text{IC}}$  and hence high fracture energies. This means that cracks will jump releasing large amounts of excess energy which is dissipated as crack branching or plastic deformation. The Talysurf traces give some clues as to the nature of the crack arrest process. Within the height resolution of the traces ( $\sim 0.01\text{ mm}$ ) it appears that considerable deviation of the cracks from the fracture plane occur and that the two halves of the fracture surface would interlock as illustrated schematically in Fig. 12. This effect could be interpreted as being due to arrest taking place by means of crack front deviation rather than more conventional blunting through plastic deformation. From the present Talysurf traces it is not possible to say whether or not plastic deformation takes place on a finer scale (below  $0.01\text{ mm}$ ).

Another feature that is apparent in under-cured samples (7.4 phr or  $50^\circ\text{C}$  post-curing) is triangular features along the arrest lines (Fig. 2a and Fig. 5a

and c). They did not occur when larger amounts of curing agent or higher post-curing temperatures were used. They were also observed in mixed-amine cured systems by Phillip *et al.* [16], who used a rather low post-cure temperature ( $60^\circ$ ). It appears that they may be caused by some type of plastic deformation or crack front deviation occurring in the under-cured resin as the crack slows down before it eventually arrests.

The other features that are commonly observed are fine markings parallel to the crack growth direction and secondary arrest lines. The origin of the secondary arrest lines is unclear. In some cases they can be correlated with slight irregularities in the load–displacement curves. They are probably due to undulations of the crack along the fracture plane and are better defined in specimens with the lower amounts of curing agent or cured for short times and at low temperatures. The fine markings were found on the fracture surfaces of most types of specimens. They usually start either from the groove in the bottom of the specimen (Fig. 2b) or from the main arrest lines (Fig. 5b). In either case, they normally terminate either before or at the next arrest line. Occasionally, they can be seen to start in neither of the two ways mentioned above and start in the middle of the fracture surface (Fig. 2b). Observations at higher magnifications show that in this case the lines are always nucleated at inhomogeneities such as foreign particles or small air bubbles.

## 5. Conclusions

It has been shown that there are many factors which control the propagation of cracks and the resulting fracture surface morphology in epoxy resins. In a DGEBA epoxy resin (Epikote 828) cured with TETA it has been found that resin cured with relatively low amounts of TETA, or with higher amounts of TETA and cured at low temperatures and for short periods of time, propagation tends to be continuous at high rates of testing, and unstable or “stick–slip” in nature at low rates of testing. Larger amounts of curing agent and higher curing temperatures tend to promote unstable propagation at all rates of testing. In a system which tends to undergo the transition when the testing rate is changed at  $20^\circ\text{C}$  (9.8 phr TETA and cured for 3 h at  $100^\circ\text{C}$ ), propagation has been found to be entirely continuous at low test temperatures (below  $0^\circ\text{C}$ ) and entirely “stick–slip” in nature above  $40^\circ\text{C}$ ,

over the range of cross-head speeds used. Also, with this material, the presence of distilled water at the crack tip is found to promote "stick-slip" propagation under conditions which would favour stable propagation in laboratory air. When fracture takes place by continuous crack propagation, the fracture surfaces are smooth and relatively featureless and it has been suggested that this is consistent with propagation taking place at a constant crack opening displacement [19]. If propagation takes place by an unstable "stick-slip" mode crack arrest lines can be seen on the surface. The intensity and the roughness of the arrest lines can be correlated with the size of the jumps. The rougher lines tend to be associated with larger jumps. During "stick-slip" propagation it appears that a constant crack opening displacement criterion does not apply. It has also been shown that there is considerable deviation of the crack from the main fracture plane at the arrest point but there is no evidence for large amounts of plastic deformation taking place even on the roughest surfaces.

## References

1. J. F. KNOTT, "Fundamentals of Fracture Mechanics" (Butterworths, London, 1973).
2. G. P. MARSHALL, L. H. COUTTS and J. G. WILLIAMS, *J. Mater. Sci.* **9** (1974) 1409.
3. P. W. R. BEAUMONT and R. J. YOUNG, *ibid.* **10** (1975) 1334.

4. R. J. YOUNG and P. W. R. BEAUMONT, *Polymer* **17** (1976) 717.
5. S. MOSTOVOY and E. J. RIPLING, *J. Appl. Polymer Sci.* **10** (1966) 1351
6. *Idem, ibid.* **13** (1969) 1083.
7. *Idem, ibid.* **15** (1971) 641.
8. *Idem, J. Appl. Polymer Symp.* **19** (1972) 395.
9. Y. M. MAI, A. G. ATKINS and R. M. CADDELL, *Int. J. Fract.* **11** (1975) 939.
10. R. A. GLEDHILL and A. J. KINLOCH, *Polymer* **17** (1976) 727.
11. R. J. YOUNG and P. W. R. BEAUMONT, *J. Mater. Sci.* **11** (1976) 776.
12. W. T. EVANS and B. I. G. BARR, *J. Strain Anal.* **9** (1974) 166.
13. A. D. S. DIGGWA, *Polymer* **15** (1974) 101.
14. D. C. PHILLIPS and J. M. SCOTT, *J. Mater. Sci.* **9** (1974) 1202.
15. K. SELBY and L. E. MILLER, *ibid.* **10** (1975) 12.
16. D. C. PHILLIPS, J. M. SCOTT and M. JONES, *ibid.* **13** (1978) 311.
17. Y. W. MAI and A. G. ATKINS, *ibid.* **10** (1975) 2000.
18. K. SELBY and L. E. MILLER, *ibid.* **10** (1975) 2003.
19. S. YAMINI, R. J. YOUNG, R. A. GLEDHILL and A. J. KINLOCH, *Polymer* **19** (1978) 574.
20. S. YAMINI and R. J. YOUNG, *ibid.* **18** (1977) 1075.
21. R. J. YOUNG and P. W. R. BEAUMONT, *J. Mater. Sci.* **12** (1977) 684.
22. A. G. ATKINS, C. S. LEE and R. M. CADDELL, *ibid.* **10** (1975) 1394.

Received 10 May and accepted 21 July 1978.